Salt-and-Pepper Noise Removal by Median-Type Noise Detectors and Detail-Preserving Regularization

Raymond H. Chan, Chung-Wa Ho, and Mila Nikolova

***Abstract*—This paper proposes a two-phase scheme for removing salt-and-pepper impulse noise. In the first phase, an adaptive median filter is used to identify pixels which are likely to be contaminated by noise (noise candidates). In the second phase, the image is restored using a specialized regularization method that applies only to those selected noise candidates. In terms of edge preservation and noise suppression, our restored images show a significant improvement compared to those restored by using just nonlinear filters or regularization methods only. Our scheme can remove salt-and-pepper-noise with a noise level as high as 90%.**

***Index Terms*—Adaptive median filter, edge-preserving regularization, impulse noise.**

I. Introduction

IMPULSE noise is caused by malfunctioning pixels in camera sensors, faulty memory locations in hardware, or transmission in a noisy channel (see [1], for instance). Two common types of impulse noise are the salt-and-pepper noise and the random-valued noise. For images corrupted by salt-and-pepper noise (respectively, random-valued noise), the noisy pixels can take only the maximum and the minimum values (respectively, any random value) in the dynamic range. There are many works on the restoration of images corrupted by impulse noise (see, for instance, the nonlinear digital filters reviewed in [2]). The median filter was once the most popular nonlinear filter for removing impulse noise because of its good denoising power [1] and computational efficiency [3]. However, when the noise level is over 50%, some details and edges of the original image are smeared by the filter [4].

Different remedies of the median filter have been proposed, e.g., the adaptive median filter [5], the multistate median filter [6], or the median filter based on homogeneity information [7], [8]. These so-called "*decision-based*" or "*switching*" filters first identify possible noisy pixels and then replace them by using the median filter or its variants, while leaving all other pixels unchanged. These filters are good at *detecting* noise even at a high noise level. Their main drawback is that the noisy pixels are replaced by some median value in their vicinity without taking into account local features such as the possible presence of edges. Hence, details and edges are not recovered satisfactorily, especially when the noise level is high.

For images corrupted by Gaussian noise, least-squares methods based on edge-preserving regularization functionals [9]–[12] have been used successfully to preserve the edges and the details in the images. These methods fail in the presence of impulse noise because the noise is heavy tailed. Moreover the restoration will alter basically all pixels in the image, including those that are not corrupted by the impulse noise. Recently, nonsmooth data-fidelity terms (e.g., ℓ_1) have been used along with edge-preserving regularization to deal with impulse noise [13].

In this paper, we propose a powerful two-stage scheme which combines the variational method proposed in [13] with the adaptive median filter [5]. More precisely, the noise candidates are first identified by the adaptive median filter, and then these noise candidates are selectively restored using an objective function with an ℓ_1 data-fidelity term and an edge-preserving regularization term. Since the edges are preserved for the noise candidates, and no changes are made to the other pixels, the performance of our combined approach is much better than that of either one of the methods. Salt-and-pepper noise with noise ratio as high as 90% can be cleaned quite efficiently.

The outline of the paper is as follows. The adaptive median filter and the edge-preserving method are reviewed in Section II. Our denoising scheme is presented in Section III. Experimental results and conclusions are presented in Sections IV and V, respectively.

II. Adaptive Median Filter and Edge-Preserving Regularization

A. Review of the Adaptive Median Filter

Let $x_{i,j}$, for $(i,j) \in \mathcal{A} \equiv \{1,\ldots,M\} \times \{1,\ldots,N\}$, be the gray level of a true M-by-N image $\mathbf{x}$ at pixel location (i,j), and $[s_{\min}, s_{\max}]$ be the dynamic range of $\mathbf{x}$, i.e., $s_{\min} \leq x_{i,j} \leq s_{\max}$ for all $(i,j) \in \mathcal{A}$. Denote by $\mathbf{y}$ a noisy image. In the classical salt-and-pepper impulse noise model, the observed gray level at pixel location (i,j) is given by

$$y_{i,j} = \begin{cases} s_{\min}, & \text{with probability } p \\ s_{\max}, & \text{with probability } q \\ x_{i,j}, & \text{with probability } 1-p-q \end{cases}$$

where $r = p + q$ defines the noise level. Here we give a brief review of the filter.

Let $S_{i,j}^w$ be a window of size $w \times w$ centered at (i,j), i.e.,

$$S_{i,j}^w = \{(k,l) : |k-i| \leq w \text{ and } |j-l| \leq w\}$$

Manuscript received November 8, 2003; revised July 30, 2004. This work was supported by HKRGC under Grant CUHK4243/01P and CUHK DAG 2060220. The associate editor coordinating the review of this manuscript and approving it for publication was Dr. Thierry Blu.

R. H. Chan and C.-W. Ho are with the Department of Mathematics, The Chinese University of Hong Kong, Shatin, Hong Kong (e-mail: rchan@math.cuhk.edu.hk; who@math.cuhk.edu.hk).

M. Nikolova is with the Centre de Mathématiques et de Leurs Applications, ENS de Cachan, 94235 Cachan Cedex, France (e-mail: nikolova@cmla.ens-cachan.fr).

Digital Object Identifier 10.1109/TIP.2005.852196

1057-7149/$20.00 © 2005 IEEE

and let $w_{\max} \times w_{\max}$ be the maximum window size. The algorithm tries to identify the noise candidates $y_{i,j}$, and then replace each $y_{i,j}$ by the median of the pixels in $S_{i,j}^{w}$.

Algorithm I (Adaptive Median Filter): For each pixel location (i,j), do the following.

1. Initialize $w = 3$.
2. Compute $s_{i,j}^{\min,w}$, $s_{i,j}^{\mathrm{med},w}$ and $s_{i,j}^{\max,w}$, which are the minimum, median, and maximum of the pixel values in $S_{i,j}^{w}$, respectively.
3. If $s_{i,j}^{\min,w} < s_{i,j}^{\mathrm{med},w} < s_{i,j}^{\max,w}$, then go to step 5. Otherwise, set $w = w + 2$.
4. If $w \leq w_{\max}$, go to step 2. Otherwise, we replace $y_{i,j}$ by $s_{i,j}^{\mathrm{med},w_{\max}}$.
5. If $s_{i,j}^{\min,w} < y_{i,j} < s_{i,j}^{\max,w}$, then $y_{i,j}$ is not a noise candidate, else we replace $y_{i,j}$ by $s_{i,j}^{\mathrm{med},w}$.

The adaptive structure of the filter ensures that most of the impulse noise are detected even at a high noise level provided that the window size is large enough. Notice that the noise candidates are replaced by the median $s_{i,j}^{\mathrm{med},w}$, while the remaining pixels are left unaltered.

B. Variational Method for Impulse Noise Cleaning

In [13], images corrupted by impulse noise are restored by minimizing a convex objective function $F_{\mathbf{y}} : \mathbb{R}^{M\times N} \to \mathbb{R}$ of the form

$$F_{\mathbf{y}}(\mathbf{u}) = \sum_{(i,j)\in\mathcal{A}} |u_{i,j} - y_{i,j}| + \frac{\beta}{2} \sum_{(i,j)\in\mathcal{A}} \sum_{(m,n)\in\mathcal{V}_{i,j}} \varphi(u_{i,j} - u_{m,n}) \quad (1)$$

where $\mathcal{V}_{i,j}$ is the set of the four closest neighbors of (i,j), not including (i,j). It was shown in [13] and [14] that, under mild assumptions and a pertinent choice of β, the minimizer $\hat{\mathbf{u}}$ of $F_{\mathbf{y}}$ satisfies $\hat{u}_{i,j} = y_{i,j}$ for most of the uncorrupted pixels $y_{i,j}$. Furthermore, all pixels $\hat{u}_{i,j}$ such that $\hat{u}_{i,j} \neq y_{i,j}$ are restored so that edges and local features are well preserved, provided that φ is an edge-preserving potential function. Examples of such functions are

$$\varphi(t) = \sqrt{\alpha + t^2}, \quad \alpha > 0$$
$$\varphi(t) = |t|^{\alpha}, \quad 1 < \alpha \leq 2$$

(see [9], [11], [15], and [16]). The minimization algorithm works on the residuals $\mathbf{z} = \mathbf{u} - \mathbf{y}$. It is sketched below.

Algorithm II:

1. Initialize $z_{ij}^{(0)} = 0$ for each $(i,j) \in \mathcal{A}$.
2. At each iteration k, calculate, for each $(i,j) \in \mathcal{A}$

$$\xi_{i,j}^{(k)} = \beta \sum_{(m,n)\in\mathcal{V}_{i,j}} \varphi'(y_{i,j} - z_{m,n} - y_{m,n})$$

where $z_{m,n}$, for $(m,n) \in \mathcal{V}_{i,j}$, are the latest updates and φ' is the derivative of φ.

TABLE I
MAXIMUM WINDOW SIZE $w_{\max}$ IN ALGORITHM I

noise level	$w_{\max} \times w_{\max}$
$r < 25\%$	5×5
$25\% \leq r < 40\%$	7×7
$40\% \leq r < 60\%$	9×9
$60\% \leq r < 70\%$	13×13
$70\% \leq r < 80\%$	17×17
$80\% \leq r < 85\%$	25×25
$85\% \leq r \leq 90\%$	39×39

3. If $\left|\xi_{i,j}^{(k)}\right| \leq 1$, set $z_{i,j}^{(k)} = 0$. Otherwise, solve for $z_{i,j}^{(k)}$ in the nonlinear equation

$$\beta \sum_{(m,n)\in\mathcal{V}_{i,j}} \varphi'(z_{i,j}^{(k)} + y_{i,j} - z_{m,n} - y_{m,n}) = \mathrm{sign}(\xi_{i,j}^{(k)}). \quad (2)$$

The updating of $z_{i,j}^{(k)}$ can be done in a red-black fashion, and it was shown in [13] that $\mathbf{z}^{(k)}$ converges to $\hat{\mathbf{z}} = \hat{\mathbf{u}} - \mathbf{y}$, where the restored image $\hat{\mathbf{u}}$ minimizes $F_{\mathbf{y}}$ in (1). If we choose $\varphi(t) = |t|^{\alpha}$, the nonlinear equation (2) can be solved by Newton's method with quadratic convergence by using a suitable initial guess derived in [17].

III. OUR METHOD

Many denoising schemes are "*decision-based*" median filters (see, for example, [6], [7], and [18]). This means that the noise candidates are first detected by some rules and are replaced by the median output or its variants. For instance, in Algorithm I, the noise candidate $y_{i,j}$, $(i,j) \in \mathcal{N}$, is replaced by $s_{i,j}^{\mathrm{med},w}$. These schemes are good because the uncorrupted pixels will not be modified. However, the replacement methods in these denoising schemes cannot preserve the features of the images, in particular the edges are smeared.

In contrast, Algorithm II can preserve edges during denoising but it has problem in detecting noisy patches, i.e., a connected region containing many noisy pixels. If one wishes to smooth out all the noisy patches, one has to increase β (see [19] for the role of β). As a result, the values of some pixels near edges will be distorted.

Combining both methods will avoid the drawbacks of either one of them. The aims of our method are to correct noisy pixels and preserve edges in the image. In the following, we denote the restored image by $\hat{\mathbf{x}}$.

Algorithm III:

1. *(Noise detection):* Denote by $\tilde{\mathbf{y}}$ the image obtained by applying an adaptive median filter to the noisy image $\mathbf{y}$. Noticing that noisy pixels take their values in the set $\{s_{\min}, s_{\max}\}$, we define the noise candidate set as

$$\mathcal{N} = \{(i,j) \in \mathcal{A} : \tilde{y}_{i,j} \neq y_{i,j} \text{ and } y_{i,j} \in \{s_{\min}, s_{\max}\}\}.$$

The set of all uncorrupted pixels is $\mathcal{N}^c = \mathcal{A} \setminus \mathcal{N}$.
2. *(Replacement):* Since all pixels in $\mathcal{N}^c$ are detected as uncorrupted, we naturally keep their original values, i.e., $\hat{x}_{i,j} = y_{i,j}$ for all $(i,j) \in \mathcal{N}^c$. Let us now consider a noise candidate, say, at $(i,j) \in \mathcal{N}$. Each one of its neighbors $(m,n) \in \mathcal{V}_{i,j}$ is either

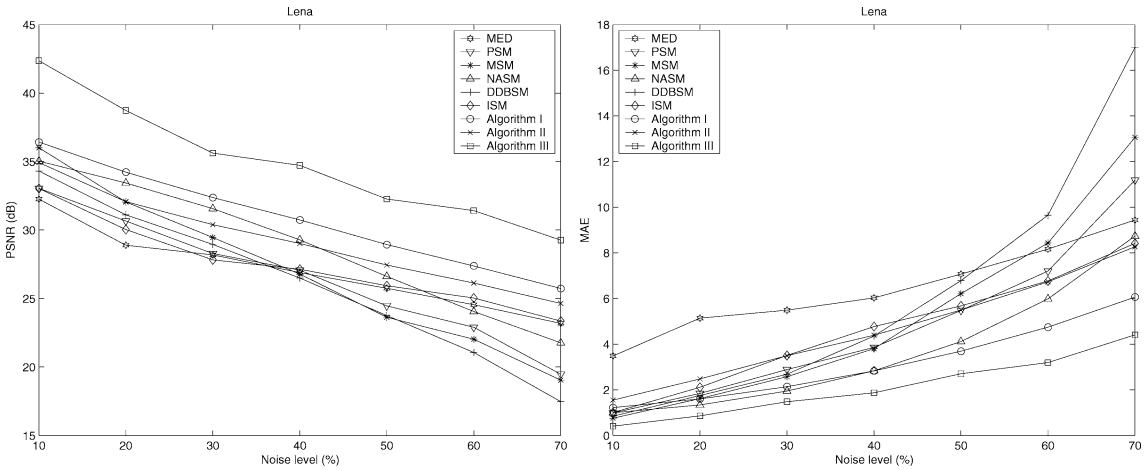

Fig. 1. Results in PSNR and MAE for the *Lena* image at various noise levels for different algorithms.

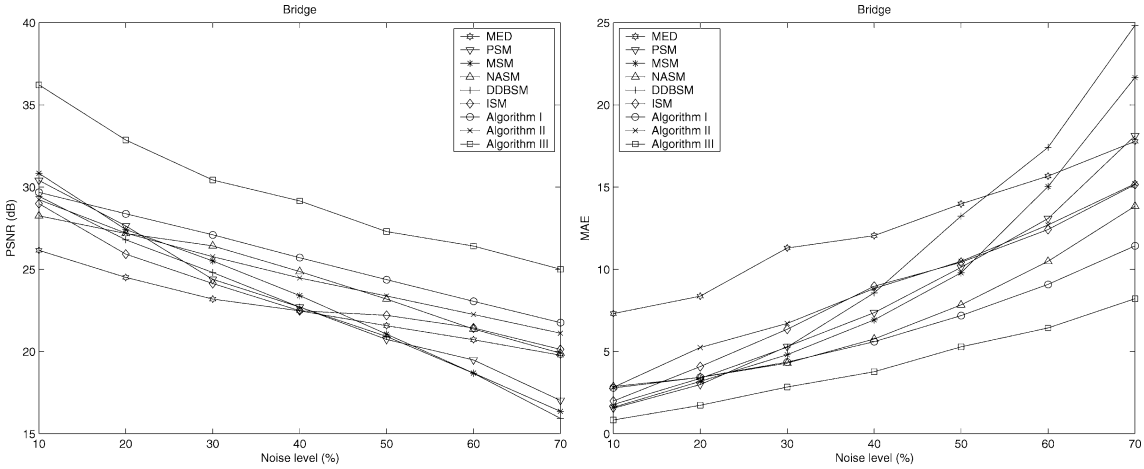

Fig. 2. Results in PSNR and MAE for the *Bridge* image at various noise levels for different algorithms.

a correct pixel, i.e., $(m,n) \in \mathcal{N}^c$ and, hence, $\hat{x}_{m,n} = y_{m,n}$; or is another noise candidate, i.e., $(m,n) \in \mathcal{N}$, in which case its value must be restored. The neighborhood $\mathcal{V}_{i,j}$ of (i,j) is, thus, split as $\mathcal{V}_{i,j} = (\mathcal{V}_{i,j} \cap \mathcal{N}^c) \cup (\mathcal{V}_{i,j} \cap \mathcal{N})$. Noise candidates are restored by minimizing a functional of the form **(1)**, but restricted to the noise candidate set $\mathcal{N}$

$$F_{\mathbf{y}}\big|_{\mathcal{N}}(\mathbf{u}) = \sum_{(i,j)\in\mathcal{N}} \left[|u_{i,j} - y_{i,j}| + \frac{\beta}{2}(S_1 + S_2) \right] \quad (3)$$

where

$$S_1 = \sum_{(m,n)\in\mathcal{V}_{i,j}\cap\mathcal{N}^c} 2 \cdot \varphi(u_{i,j} - y_{m,n})$$

$$S_2 = \sum_{(m,n)\in\mathcal{V}_{i,j}\cap\mathcal{N}} \varphi(u_{i,j} - u_{m,n}).$$

The restored image $\hat{\mathbf{x}}$ with indices $(i,j) \in \mathcal{N}$ is the minimizer of **(3)** which can be obtained by using Algorithm II but restricted onto $\mathcal{N}$ instead of onto $\mathcal{A}$. As in **(1)**, the ℓ_1 data-fidelity term $|u_{i,j} - y_{i,j}|$ discourages those wrongly detected uncorrupted pixels in $\mathcal{N}$ from being modified to other values. The regularization term $(S_1 + S_2)$ performs edge-preserving smoothing for the pixels indexed by $\mathcal{N}$.

Let us emphasize that Step 1 of our method can be realized by any reliable impulse noise detector, such as the multistate median filter [6] or the improved detector [18], etc. Our choice, the adaptive median filter, was motivated by the fact that it provides a good compromise between simplicity and robust noise detection, especially for high level noise ratios. The pertinence of this choice can be seen from the experimental results in [20] (where the noise level is 50%) or Figs. 3(h) and 4(h) (where the noise level is 70%).

IV. Simulations

A. Configuration

Among the commonly tested 512 × 512 8-bit grayscale images, the one with homogeneous region (*Lena*) and the one with high activity (*Bridge*) will be selected for our simulations. Their dynamic ranges are [0, 255]. In the simulations, images will be corrupted by "salt" (with value 255) and "pepper" (with value 0)

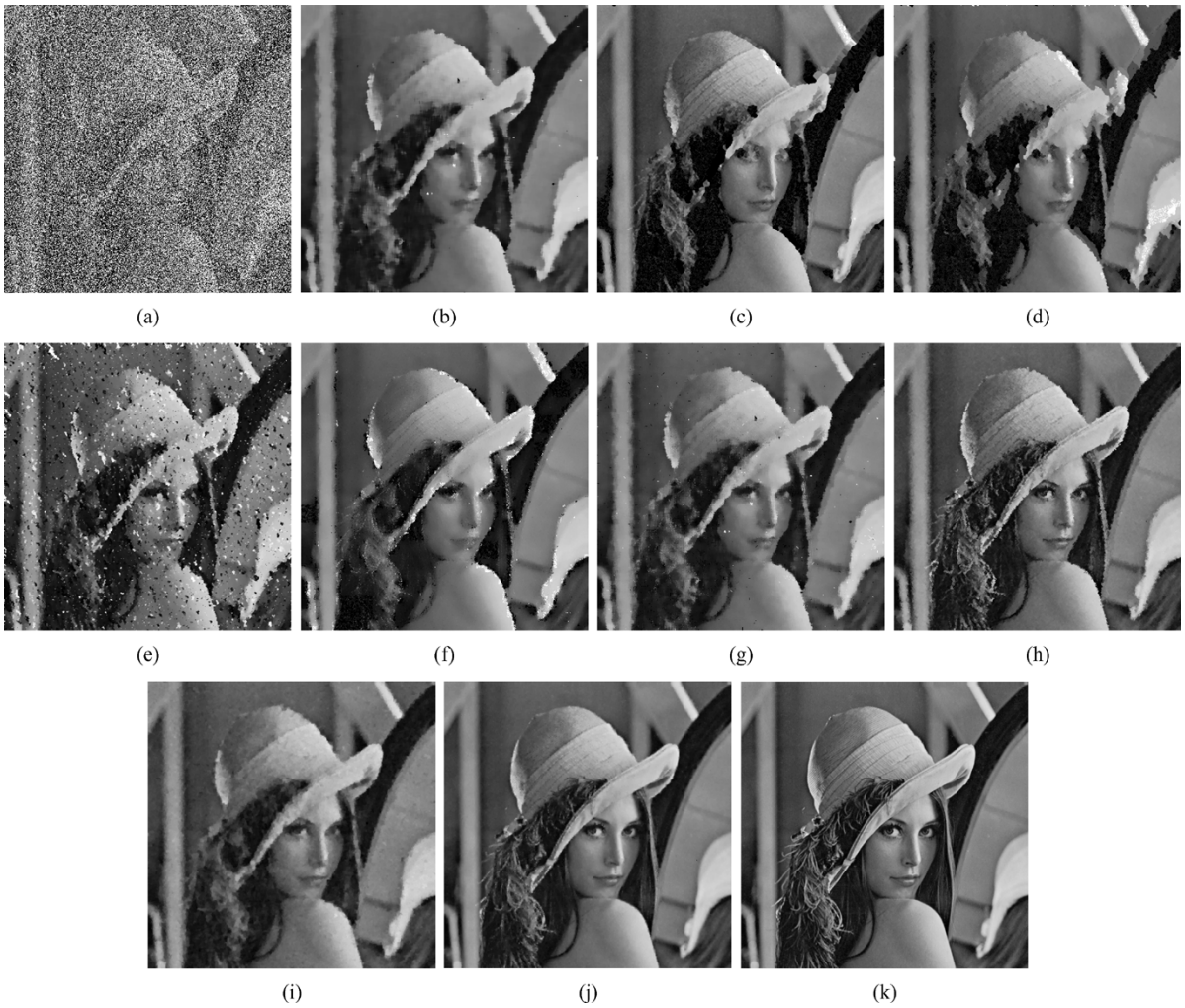

Fig. 3. Restoration results of different filters. (a) Corrupted *Lena* image with 70% salt-and-pepper noise (6.7 dB). (b) MED filer (23.2 dB). (c) PSM filter (19.5 dB). (d) MSM filter (19.0 dB). (e) DDBSM filter (17.5 dB). (f) NASM filter (21.8 dB). (g) ISM filter (23.4 dB). (h) Algorithm I (25.8 dB). (i) Algorithm II (24.6 dB). (j) Our proposed algorithm (29.3 dB). (k) Original image.

noise with equal probability. Also a wide range of noise levels varied from 10% to 70% with increments of 10% will be tested. Restoration performances are quantitatively measured by the peak signal-to-noise ratio (PSNR) and the mean absolute error (MAE) defined in [1, p. 327]

$$\mathrm{PSNR} = 10\log_{10}\frac{255^2}{\frac{1}{MN}\sum_{i,j}(r_{i,j}-x_{i,j})^2}$$

$$\mathrm{MAE} = \frac{1}{MN}\sum_{i,j}|r_{i,j}-x_{i,j}|$$

where $r_{i,j}$ and $x_{i,j}$ denote the pixel values of the restored image and the original image, respectively.

For Algorithm I (the adaptive median filter), the maximum window size $w_{\max}$ should be chosen such that it increases with the noise level in order to filter out the noise. Since it is not known *a priori*, we tried different $w_{\max}$ for any given noise level, and found that $w_{\max}$ given in Table I are sufficient for the filtering. We, therefore, set $w_{\max} = 39$ in all our tests. We remark that with such choice of $w_{\max}$, almost all the salt-and-pepper noise are detected in the filtered images.

For Algorithm II (the variational method in [13]), we choose $\varphi(t) = |t|^\alpha$ as the edge-preserving function. We observe that if α is small ($1 < \alpha < 1.1$), most of the noise is suppressed but staircases appear. If α is large ($\alpha > 1.5$), the fine details are not distorted seriously but the noise cannot be fully suppressed. The selection of α is a tradeoff between noise suppression and detail preservation [13]. In the tests, the best restoration results are not sensitive to α when it is between 1.2 and 1.4. We, therefore, choose $\varphi(t) = |t|^{1.3}$, and β is tuned to give the best result in terms of PSNR.

For our proposed Algorithm III, the noise candidate set $\mathcal{N}$ should be obtained such that most of the noise are detected. This, again, amounts to the selection of $w_{\max}$. As mentioned, $w_{\max} = 39$ can be fixed for most purposes. Then, we can restore those noise pixels $y_{i,j}$ with $(i,j) \in \mathcal{N}$. As in Algorithm II, the edge-preserving function $\varphi(t) = |t|^{1.3}$ will be used. That leaves only the parameter β to be determined. Later, we will demonstrate that our proposed algorithm is very robust with respect to β, and, thus, we fix $\beta = 5$ in all the tests.

For comparison purpose, Algorithm I, Algorithm II, the standard median (MED) filter, and, also, recently proposed filters like the progressive switching median (PSM) filter [21],

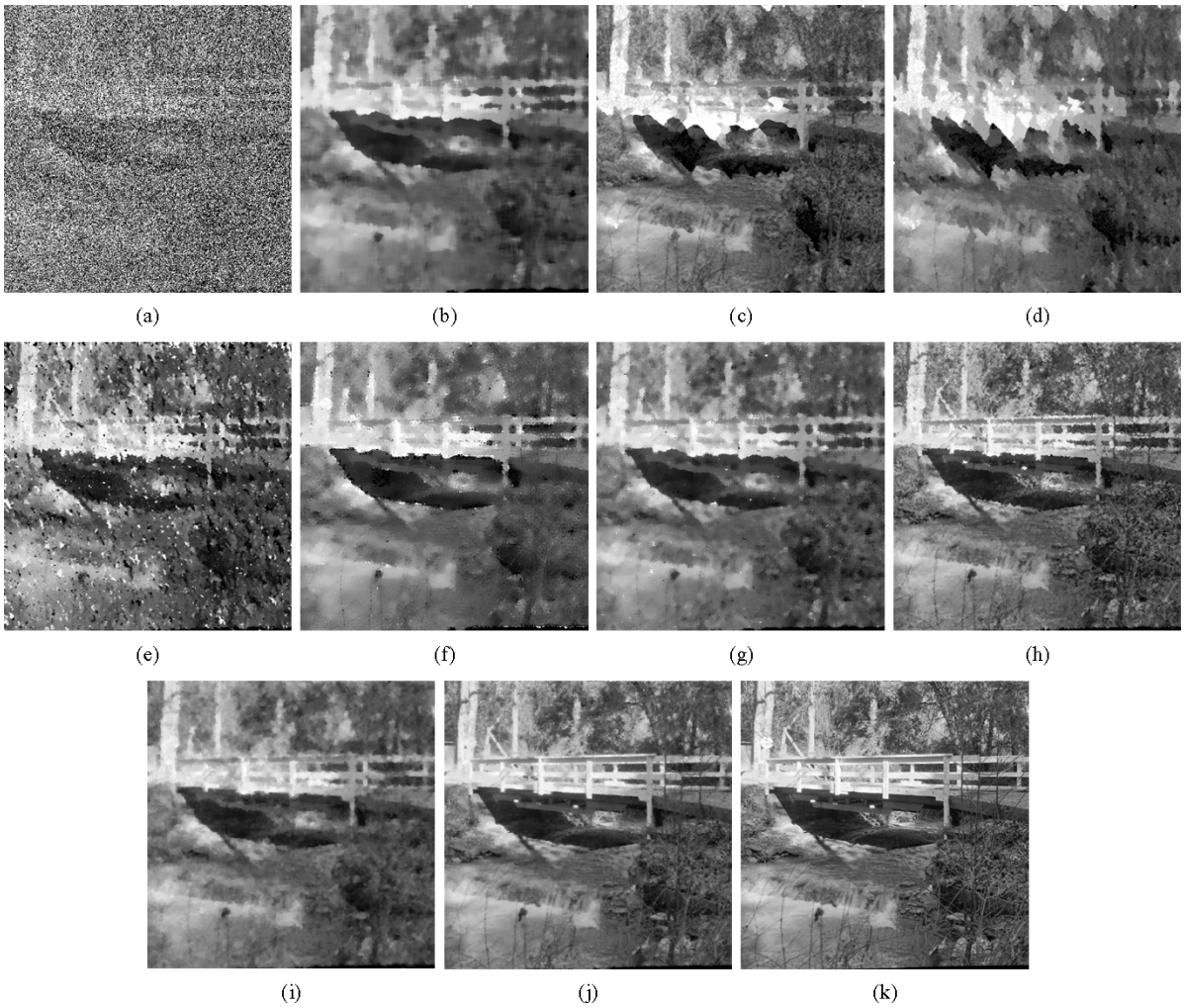

Fig. 4. Restoration results of different filters: (a) Corrupted *Bridge* image with 70% salt-and-pepper noise (6.8 dB). (b) MED filer (19.8 dB). (c) PSM filter (17.0 dB). (d) MSM filter (16.4 dB). (e) DDBSM filter (15.9 dB). (f) NASM filter (19.9 dB). (g) ISM filter (20.1 dB). (h) Algorithm I (21.8 dB). (i) Algorithm II (21.1 dB). (j) Our proposed algorithm (25.0 dB). (k) Original image.

the multistate median (MSM) filter [6], the noise adaptive soft-switching median (NASM) filter [7], the directional difference-based switching median (DDBSM) filter [22], and the improved switching median (ISM) filter [18] are also tested. For the MED filter, the window sizes are chosen for each noise level to achieve its best performance. For the MSM filter, the maximum center weights of 7, 5, and 3 are tested for each noise level. For the ISM filter, the convolution kernels K_5, K_7 and K_9 and filtering window sizes of 9×9 and 11×11 are used. The decision thresholds in the PSM, MSM, DDBSM, ISM filters are also tuned to give the best performance in terms of PSNR.

B. Denoising Performance

We summarize the performance of different methods in Figs. 1 and 2. From the plots, we see that all the methods have similar performance when the noise level is low. This is because those recently proposed methods focus on the noise detection. However, when the noise level increases, noise patches will be formed and they may be considered as noise free pixels. This causes difficulties in the noise detection algorithm. With erroneous noise detection, no further modifications will be made to the noise patches, and, hence, their results are not satisfactory.

On the other hand, our proposed denoising scheme achieves a significantly high PSNR and low MAE even when the noise level is high. This is mainly based on the accurate noise detection by the adaptive median filter and the edge-preserving property of the variational method of [13].

In Figs. 3 and 4, we present restoration results for the 70% corrupted *Lena* and *Bridge* images. Among the restorations, except for our proposed one, Algorithm I gives the best performance in terms of noise suppression and detail preservation. As mentioned before, it is because the algorithm locates the noise accurately. In fact, about 70.2% and 70.4% pixels are detected as noise candidates in *Lena* and *Bridge*, respectively, by Algorithm I. However, the edges are jittered by the median filter. For Algorithm II, much of the noise is suppressed but the blurring and distortion are serious. This is because every pixel has to be examined and may have been altered. Compared with all the algorithms tested, our proposed Algorithm III is the best one. It has successfully suppressed the noise with the details and the edges of the images being preserved very accurately.

(a) (b) (c) (d)

Fig. 5. Restorations of 90% corrupted images: (a) *Lena* by Algorithm I (21.1 dB). (b) *Lena* by Algorithm III (25.4 dB). (c) *Bridge* by Algorithm I (18.1 dB). (d)*Bridge* by Algorithm III (21.5 dB).

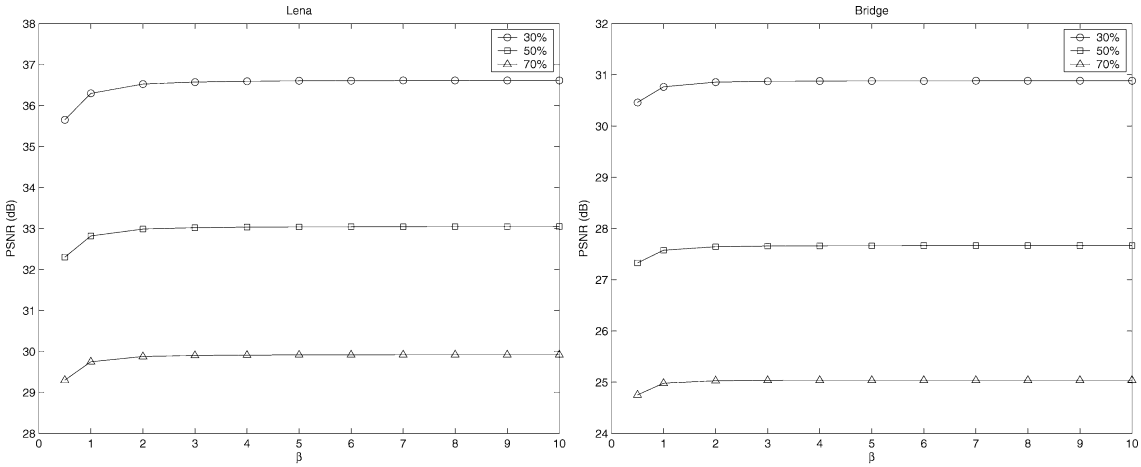

(a) (b)

Fig. 6. PSNR of restored images by our Algorithm III for different β. (a) *Lena* image. (b) *Bridge* image.

Finally, to demonstrate the excellent performance of our proposed filter, 90% corrupted *Lena* and *Bridge* are restored by Algorithm I and by our Algorithm III (see Fig. 5). We can clearly see the visual differences and also the improvement in PSNR by using our algorithm.

C. Robustness With Respect to β

For Algorithm II, the choice of β is crucial in the restoration. To show that our Algorithm III is robust with respect to β, $0.5 \leq \beta \leq 10$ are tested for noise levels 30%, 50%, and 70% (see Fig. 6). From the plots, we see that the PSNR is very stable when $1 \leq \beta \leq 10$. Hence, one can set $\beta = 5$ for all denoising problems in practice. If one further use $\varphi(t) = |t|^{1.3}$ as we did in our tests, and set $w_{\max} = \min\{M, N\}$ (which will be able to detect all salt-and-pepper noise), then our algorithm is parameter free.

D. Computational Complexity

We end this section by considering the complexity of our algorithm. Our algorithm requires two phases: noise detection and replacement. Noise detection is done by Algorithm I, the adaptive median filter. Like other median-type filters, it is relatively fast. Although $w_{\max}$ may be quite large, the loop in Algorithm I is automatically stopped at step 3 when the noise level is not high. The replacement step is the most time-consuming part of our algorithm as it requires the minimization of the functional in (3). It is equivalent to solving the nonlinear equation (2) for each pixel in the noise candidate set (see [17]). In Table II, we compare the CPU time needed for all three algorithms when MATLAB 6.5 (R13) is used on a PC equipped with an AMD 1.8-GHz CPU and 224-MB RAM memory. We see that our Algorithm III is about 20–90 times slower than Algorithm I.

TABLE II
COMPARISON OF CPU TIME IN SECONDS

Image	Noise level	Algo. I	Algo. II	Algo. III
Lena	70%	23	6865	2009
	90%	311	> 12000	6917
Bridge	70%	56	8003	4263
	90%	311	> 12000	10070

We emphasize, however, that the main contribution of our paper is a method that is capable of restoring images corrupted by salt-and-pepper noise with extremely high noise ratio. Our method can be used as a post-processing image enhancement procedure that improves on the images obtained by fast algorithms such as the adaptive median filter, or as a preprocessing procedure that cleans up images before dimensionality reduction in data mining [24].

Our computational cost can be reduced further by better implementations of minimization routines for solving (3) (see, for example, the continuation method [10] and the primal-dual formulation [23] for TV minimization).

V. Conclusion

In this paper, we propose a decision-based, detail-preserving restoration method. It is the ultimate filter for removing salt-and-pepper noise. Experimental results show that our method performs much better than median-based filters or the edge-preserving regularization methods. Even at a very high noise level ($\leq 90\%$), the texture, details, and edges are preserved accurately. One can further improve our results by using different noise detectors and regularization functionals that are tailored to different types of noises, such as the random-valued impulse noise or impulse-plus-Gaussian noise. These extensions together with fast solvers for (3) will be given in our forthcoming papers.

References

[1] A. Bovik, *Handbook of Image and Video Processing*. New York: Academic, 2000.

[2] J. Astola and P. Kuosmanen, *Fundamentals of Nonlinear Digital Filtering*. Boca Raton, FL: CRC, 1997.

[3] T. S. Huang, G. J. Yang, and G. Y. Tang, "Fast two-dimensional median filtering algorithm," *IEEE Trans. Acoustics, Speech, Signal Process.*, vol. ASSP-1, no. 1, pp. 13–18, Jan. 1979.

[4] T. A. Nodes and N. C. Gallagher, Jr., "The output distribution of median type filters," *IEEE Trans. Commun.*, vol. COM-32, no. 5, pp. 532–541, May 1984.

[5] H. Hwang and R. A. Haddad, "Adaptive median filters: New algorithms and results," *IEEE Trans. Image Process.*, vol. 4, no. 4, pp. 499–502, Apr. 1995.

[6] T. Chen and H. R. Wu, "Space variant median filters for the restoration of impulse noise corrupted images," *IEEE Trans. Circuits Syst. II, Analog Digit. Signal Process.*, vol. 48, no. 8, pp. 784–789, Aug. 2001.

[7] H.-L. Eng and K.-K. Ma, "Noise adaptive soft-switching median filter," *IEEE Trans. Image Process.*, vol. 10, no. 2, pp. 242–251, Feb. 2001.

[8] G. Pok, J.-C. Liu, and A. S. Nair, "Selective removal of impulse noise based on homogeneity level information," *IEEE Trans. Image Process.*, vol. 12, no. 1, pp. 85–92, Jan. 2003.

[9] S. Z. Li, "On discontinuity-adaptive smoothness priors in computer vision," *IEEE Trans. Pattern Anal. Mach. Intell.*, vol. 17, no. 6, pp. 576–586, Jun. 1995.

[10] T. F. Chan, H. M. Zhou, and R. H. Chan, "A continuation method for total variation denoising problems," in *Proc. SPIE Symp. Advanced Signal Processing: Algorithms, Architectures, and Implementations*, vol. 2563, F. T. Luk, Ed., 1995, pp. 314–325.

[11] P. Charbonnier, L. Blanc-Féraud, G. Aubert, and M. Barlaud, "Deterministic edge-preserving regularization in computed imaging," *IEEE Trans. Image Process.*, vol. 6, no. Mar., pp. 298–311, 1997.

[12] C. R. Vogel and M. E. Oman, "Fast, robust total variation-based reconstruction of noisy, blurred images," *IEEE Trans. Image Process.*, vol. 7, no. Jun., pp. 813–824, 1998.

[13] M. Nikolova, "A variational approach to remove outliers and impulse noise," *J. Math. Imag. Vis.*, vol. 20, pp. 99–120, 2004.

[14] ——, "Minimizers of cost-functions involving nonsmooth data-fidelity terms. Application to the processing of outliers," *SIAM J. Numer. Anal.*, vol. 40, pp. 965–994, 2002.

[15] M. Black and A. Rangarajan, "On the unification of line processes, outlier rejection, and robust statistics with applications to early vision," *Int. J. Comput. Vis.*, vol. 19, pp. 57–91, 1996.

[16] P. J. Green, "Bayesian reconstructions from emission tomography data using a modified EM algorithm," *IEEE Trans. Med. Imag.*, vol. MI-9, no. 1, pp. 84–93, Jan. 1990.

[17] R. H. Chan, C.-W. Ho, and M. Nikolova, "Convergence of Newton's method for a minimization problem in impulse noise removal," *J. Comput. Math.*, vol. 22, pp. 168–177, 2004.

[18] S. Zhang and M. A. Karim, "A new impulse detector for switching median filters," *IEEE Signal Process. Lett.*, vol. 9, no. 11, pp. 360–363, Nov. 2002.

[19] T. F. Chan and S. Esedoglu, "Aspects of total variation regularized L^1 function approximation," Dept. Math., Univ. California, Los Angeles, CAM Rep. (04-07), 2004.

[20] R. C. Gonzalez and R. E. Woods, *Digital Image Processing*, 2nd ed. Upper Saddle River, NJ: Prentice-Hall, 2001.

[21] Z. Wang and D. Zhang, "Progressive switching median filter for the removal of impulse noise from highly corrupted images," *IEEE Trans. Circuits Syst. II., Analog Digit. Signal Process.*, vol. 46, no. 1, pp. 78–80, Jan. 1999.

[22] Y. Hashimoto, Y. Kajikawa, and Y. Nomura, "Directional difference-based switching median filters," *Electron. Commun. Jpn.*, vol. 85, pp. 22–32, 2002.

[23] T. F. Chan, G. H. Golub, and P. Mulet, "A nonlinear primal-dual method for total variation-based image restoration," *SIAM J. Sci. Comput.*, vol. 20, pp. 1964–1977, 1999.

[24] E. Bingham and H. Mannila, "Random projection in dimensionality reduction: Applications to image and text data," in *Proc. 7th ACM SIGKDD Int. Conf. Knowledge Discovery and Data Mining (KDD-2001)*, San Francisco, CA, Aug. 26-29, 2001, pp. 245–250.

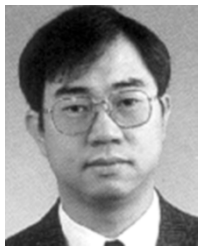

Raymond H. Chan is a Professor in the Department of Mathematics, Chinese University of Hong Kong. His research interests include numerical linear algebra and image processing problems.

Chung-Wa Ho was born on January 9, 1980 in Hong Kong. He received the B.Sc. and M.Phil. degrees in mathematics from the Chinese University of Hong Kong in 2002 and 2004, respectively.

His research area includes image processing and numerical analysis.

Mila Nikolova is a Researcher with the National Center for Scientific Research (CNRS), France, and is currently with the Center for Mathematics and their Applications (CMLA), ENS de Cachan, France. Her research interests include inverse problems, mathematical image and signal processing, and variational problems and their analysis.